Bukovinian Math. Journal. 2025, **13**, 2, 188–200 Буковинський матем. журнал 2025, Т.13, №2, 188–200

DOI: https://doi.org/10.31861/bmj2025.02.19

Grigorchuk R.I., Samarakoon S.T., Vorobets Y.

ON THE SECOND 2-DIMENSIONAL RATIONAL MAP ASSOCIATED WITH THE FIRST GROUP OF INTERMEDIATE GROWTH

We show that the second rational map G associated with the group $\mathcal{G}$ of intermediate growth constructed by the first author in 1980 is semiconjugate with the antiholomorphic map $z \to \bar{z}^2$. For doing this we use a family of G–invariant curves found by the third author and for each invariant curve, create a Markov partition of it.

Key words and phrases: Grigorchuk Group, Intermediate Growth, Complex Dynamics, Markov Shift.

Texas A&M University, College Station, Texas, United States (Grigorchuk R.I.)
Sam Houston State University, Huntsville, Texas, United States (Samarakoon S.T.)
Texas A&M University, College Station, Texas, United States (Vorobets Y.)
e-mail: *grigorch@tamu.edu (Grigorchuk R.I.), ssamarakoon@shsu.edu (Samarakoon S.T.), yvorobets@tamu.edu (Vorobets Y.)*

Introduction

The dynamics of rational maps has attracted sustained interest due to its central role in complex dynamics and its deep connections with diverse areas of mathematics. Iteration of rational maps on the Riemann sphere exhibits a rich interplay between stability and chaos, captured by the dichotomy between the Fatou and Julia sets [5, 12]. Beyond its intrinsic dynamical complexity, the study of rational maps has strong links to holomorphic dynamics, potential theory, and geometric function theory [16]. It also interfaces with number theory through arithmetic dynamics, where questions about periodic points, canonical heights, and equidistribution have led to significant advances [19]. Moreover, rational maps serve as fundamental models for nonlinear phenomena, making them a natural testing ground for general concepts in ergodic theory and bifurcation theory [14].

Multidimensional rational maps associated with graphs and groups have become an important tool for analyzing self-similar and recursively defined structures. In the context of self-similar and automaton groups, the recursive action on rooted trees gives rise to natural renormalization schemes that can be encoded by rational maps acting on finite-dimensional parameter spaces [6, 7, 17]. Such renormalization maps play a central role in the spectral analysis of Schreier graphs and Hecke-type operators for fractal groups, where iteration of rational maps governs the asymptotic behavior of spectra and Green functions [2, 4]. Closely related ideas appear in the study of Laplacians

УДК 514.7:512
2010 *Mathematics Subject Classification:* 20E08, 37D20.

© Grigorchuk R.I., Samarakoon S.T., Vorobets Y., 2025

on self-similar graphs and lattices, where spectral decimation leads to multidimensional rational maps whose dynamics control eigenvalue distributions and spectral measures [21, 18, 1, 22]. These methods also interact with probabilistic and geometric aspects of groups, including random walks and amenability, where self-similarity and renormalization phenomena are fundamental [3, 13, 8].

The study of growth rates of groups has a long history [20, 15, 11], and it is well known that such growth can range from polynomial to exponential, with intermediate growth lying strictly between these two extremes. The first example of a group of intermediate growth – neither polynomial nor exponential – was constructed by the first author in 1980 [9]. This group, $\mathcal{G}$, is a finitely generated infinite torsion group, and it was subsequently shown in [10] that its growth is indeed intermediate.

The group $\mathcal{G}$ is associated with two 2–dimensional rational maps given below:

$$F\colon \begin{pmatrix} x \\ y \end{pmatrix} \mapsto \begin{pmatrix} \dfrac{2x^2}{4-y^2} \\ y + \dfrac{x^2 y}{4-y^2} \end{pmatrix}$$

$$G\colon \begin{pmatrix} x \\ y \end{pmatrix} \mapsto \begin{pmatrix} \dfrac{2(4-y^2)}{x^2} \\ -y - \dfrac{y(4-y^2)}{x^2} \end{pmatrix} \tag{1}$$

Both maps share many properties such as topological and algebraic degrees, indeterminacy points, and algebraic stability [4]. The map F has been studied extensively in the literature (see [4]), whereas the corresponding map G has received comparatively little attention to date. It is know that the map G semiconjugate to the Ulam-Chebyshev map.

Theorem 1 ([6]). *The maps F and G are semiconjugate to the Ulam-Chebyshev map $z \mapsto 2z^2 - 1$ and hence to $z \mapsto z^2$, via the rational functions $\psi_F\colon (x, y) \mapsto \dfrac{4 - x^2 + y^2}{4y}$ and $\psi_G\colon (x, y) \mapsto \dfrac{4 + x^2 - y^2}{4x}$, respectively.*

The maps F and G are two dimensional versions of more complicated maps in $\mathbb{C}^4$ computed by V.Nekrashevych and the first author in [6] using the Schur map technique that they extended to the case of self–similar C*–algebras acting in infinite–dimensional Hilbert space.

In this article, we continue investigating the map G and its dynamical properties. It is observed by the third author that the rational function I, defined by

$$I(x, y) = -\frac{\left(x^6 - x^4y^2 - 12x^4 - 4x^2y^2 + 48x^2 - 4y^4 + 32y^2 - 64\right)^2}{\left(x^4 - 8x^2 - 4y^2 + 16\right)^2 \left(x^4 - 2x^2y^2 - 8x^2 + y^4 - 8y^2 + 16\right)}, \tag{2}$$

is invariant under the map G. Consequently, the level curves $I = c$, denoted by I_c, are G–invariant. In particular, the invariant curves I_0, I_∞, and I_2 are presented in Figure 1. Further examination of the level curves I_c shows that each I_c consists of two disjoint components, which we denote by I_c^1 and I_c^2. Moreover, each component admits a natural partition into twelve sub–arcs. This decomposition allows for a more refined analysis of the restriction of G to the invariant curves I_c and reveals additional structure in the dynamics. As a result, we obtain the following theorem.

Theorem 2. *1. The map G has a family of invariant curves I_c given by the equation $I(x, y) = c$, $c \in \mathbb{R}$, where $I(x, y)$ is the rational function given by Equation (2). Each curve I_c consists of two disjoint components I_c^1 and I_c^2.*

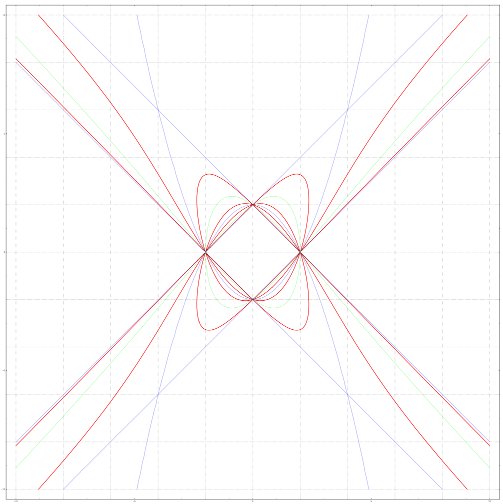

Figure 1: Red: $I = 2$, Green: $I = 0$, Blue: $I = \infty$

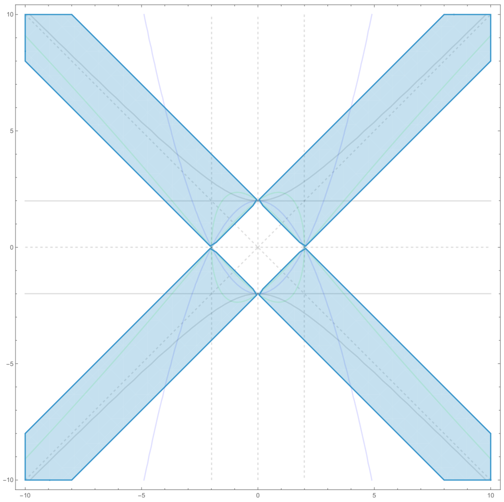

Figure 2: The *cross*, R_C, defined using four straight lines with slopes ± 1 and intercepts $(0, \pm 2)$ is given by $R_C = \{(x, y) \in \mathbb{R}^2 | (x + y + 2)(x + y - 2)(x - y + 2)(x - y - 2) < 0\}$.

2. *For $i \in \{1, 2\}$, the dynamics of the restriction of G on I_c^i is determined by the Markov partition consisting of 12 pieces and hence $G|_{I_c^i}$ from the dynamical point of view is a Markov shift.*

3. *For $i \in \{1, 2\}$, G restricted to I_c^i is semiconjugate to the antiholomorphic map $z \mapsto \bar{z}^2$.*

The cross-shaped structure

$$R_C = \left\{(x, y) \in \mathbb{R}^2 | (x + y + 2)(x + y - 2)(x - y + 2)(x - y - 2) < 0\right\}$$

(hereafter referred to simply as the *cross*), shown in Figure 2, happens to be crucial in calculating the joint spectrum of a family of operators arising from the group $\mathcal{G}$ [2, 1, 6, 4]. The level curves I_c forms a foliation of the cross when $c \geq 0$ and a foliation of the exterior of the cross when $c \leq -1$, as seen in the Figure 3.

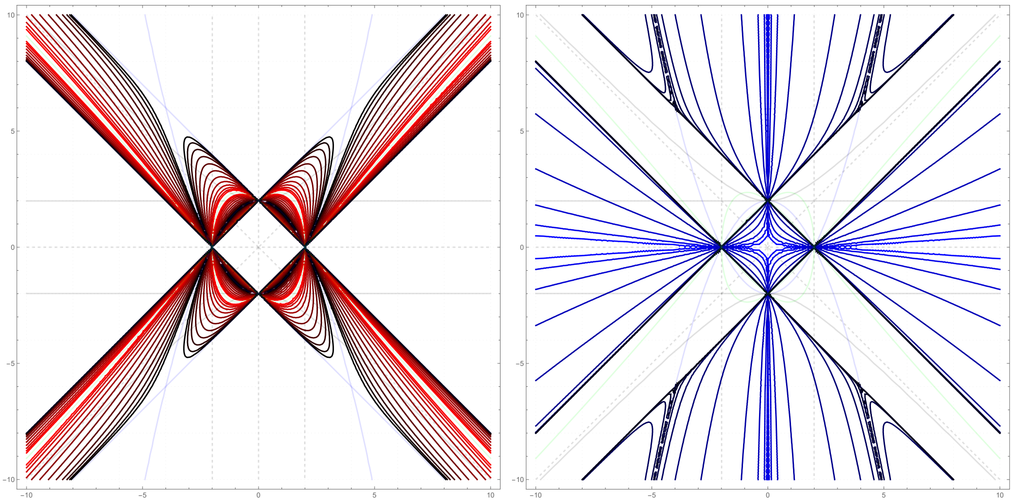

(a) (b)

Figure 3: Foliation of the plane by G–invariant curves I_c. Figure 3a illustrates the foliation of the interior of the cross when $c \geq 0$ and Figure 3b illustrates the foliation of the exterior of the cross when $c \leq -1$.

1 The map G and G–invariant function I

We dedicate this section to the study of the properties of the map G (defined in Equation (1)) and the function I (defined in Equation (2)). First, let us observe some properties of the map G.

Proposition 1. *1. The map G has topological degree 2 and algebraic degree 3.*

2. The vertical axis is mapped to infinity, except for the points $(0, \pm 2)$, which are indertminacy points of G.

3. The map G is symmetric in the first coordinate and skew–symmetric in the second coordinate. That is, if $(X, Y) = G(x, y)$, then $G(-x, y) = (X, Y)$ and $G(x, -y) = (X, -Y)$.

We now consider the rational function I defined in Equation (2). Observe that its denominator admits a factorization, allowing the map I to be rewritten in the following form:

$$I(x, y) = -\frac{\left(x^6 - x^4y^2 - 12x^4 - 4x^2y^2 + 48x^2 - 4y^4 + 32y^2 - 64\right)^2}{\left(x^2 + 2y - 4\right)^2 \left(x^2 - 2y - 4\right)^2 (x + y + 2)(x + y - 2)(x - y + 2)(x - y - 2)}.$$

Next, we introduce a set of functions that will be instrumental in analyzing the function I. First, we define the linear functions

$$\begin{aligned} L_{+,+}(x,y) &:= L_{+,+} := x + y + 2, & L_{+,-}(x,y) &:= L_{+,-} := x + y - 2, \\ L_{-,+}(x,y) &:= L_{-,+} := x - y + 2, & L_{-,-}(x,y) &:= L_{-,-} := x - y - 2, \\ H_{+}(x,y) &:= H_{+} := y + 2, & H_{-}(x,y) &:= H_{-} := y - 2, \end{aligned} \tag{3}$$

that describe a family of straight lines. Then, we define quadratic polynomials

$$P_{+}(x,y) := P_{+} := x^2 + 2y - 4, \qquad P_{-}(x,y) := P_{-} := x^2 - 2y - 4, \tag{4}$$

defining parabolic curves,

$$H(x,y) := H := x^2 - y^2 + 4, \tag{5}$$

which characterizes a hyperbola, and a degree six polynomial

$$N(x,y) := N = \left(x^6 - x^4y^2 - 12x^4 - 4x^2y^2 + 48x^2 - 4y^4 + 32y^2 - 64\right). \tag{6}$$

They will serve as a foundational framework for subsequent geometric and analytical discussions. The following proposition describes the image of these polynomials under the map G.

Proposition 2. *Let (X,Y) denote the image of (x,y) under the map G. Then;*

1. $X = -\frac{2}{x^2}H_+H_-.$
2. $Y = -\frac{y}{x^2}H.$
3. $N(X,Y) = -\frac{4}{x^{12}}NH^3H_+^2H_-^2.$
4. $H(X,Y) = -\frac{1}{x^4}H_+H_- \cdot (x^4 - 2x^2y^2 + y^4 - 8y^2 + 16).$
5. $P_+(X,Y) = -\frac{2}{x^4}HP_+H_+.$
6. $P_-(X,Y) = \frac{2}{x^4}HP_-H_-.$
7. $L_{+,+}(X,Y) = -\frac{1}{x^2}HH_-.$
8. $L_{+,-}(X,Y) = -\frac{1}{x^2}L_{+,-}L_{-,+}H_+.$
9. $L_{-,+}(X,Y) = \frac{1}{x^2}HH_+.$
10. $L_{-,-}(X,Y) = \frac{1}{x^2}L_{+,+}L_{-,-}H_-.$
11. $H_+(X,Y) = -\frac{1}{x^2}H_- \cdot (x^2 - y^2 - 2y).$
12. $H_-(X,Y) = -\frac{1}{x^2}H_+ \cdot (x^2 - y^2 + 2y).$

Using the polynomials in (3), (4), and (6) we write the ration function I as

$$I(x,y) = -\frac{N^2}{P_+^2P_-^2L_{+,+}L_{+,-}L_{-,+}L_{-,-}}. \tag{7}$$

Applying Proposition 2 to the Equation (7) shows that the rational function I is G–invariant, which is restated below.

Theorem 3. *The rational function I is G–invariant. That is, $I(G(x,y)) = I(x,y)$ on the set of points where the function I is defined.*

The set of indeterminacies of I occurs when both the numerator and the denominator of I vanish simultaneously, which happened to be the set $\{(\pm 2,0),(0,\pm 2)\}$. Beside from the indeterminacy points, the points where the numerator, N, vanishes coincide with the roots of the map I. This shows that the roots of I lie in the cross, R_C that is shown in Figure 2. The cross can be written using the polynomials from (3) as

$$R_C = \left\{(x,y) \in \mathbb{R}^2 | L_{+,+}L_{-,+}L_{+,-}L_{-,-} < 0\right\}.$$

Note that a point (x,y) lies inside the cross is equivalent to the condition that the denominator in Equation (7) is less than zero, which is equivalent to the condition that $I(x,y) \geq 0$. Thus, the points that lie inside the cross can be characterized by $I \geq 0$. We summarize this more formally in the following proposition.

Proposition 3. *Let (x,y) be a non–indeterminacy point of I that does not lie on parabolas $P_+ = 0$ and $P_- = 0$. Then,*

1. *The point (x,y) is on the boundary of the cross if and only if $I(x,y)$ is infinite.*
2. *The point (x,y) is in the cross if and only if $I(x,y) \geq 0$.*
3. *The point (x,y) is in the exterior of the cross if and only if $I(x,y) < 0$.*

2 Invariant Curves I_c

Let I_c be the curves $I(x,y) = c$, where $c \in [0,\infty]$. By the Theorem 3, the curves I_c are G–invariant. The invariant curves I_0, I_∞, and I_2 are presented in Figure 1. From this point onward, we will use the curve I_2 as a tool for visualizing the structure and behavior of I_c. By Proposition 3, we see that I_c lies in the cross for $c \geq 0$. Thus, we restrict our analysis to the cross R_C.

To study the invariant curves I_c, we partition the cross R_C into 24 parts using functions N, P_+, P_-, H, defined by Equations (4),(5), and (6), x, and y. The partition of R_C is shown in Figure 4.

$$\begin{aligned}
R_1 &:= \{(x,y) \in R_C | N < 0, P_+ < 0, xP_- < 0, xH > 0, y < 0\},\\
R_2 &:= \{(x,y) \in R_C | N < 0, P_+ < 0, P_- > 0, H > 0, x < 0\},\\
R_3 &:= \{(x,y) \in R_C | N > 0, P_+ > 0, P_- < 0, H > 0, x < 0\},\\
R_4 &:= \{(x,y) \in R_C | N > 0, xP_+ < 0, xH > 0, y > 0\},\\
R_5 &:= \{(x,y) \in R_C | N < 0, P_+ > 0, H > 0, L_{-,-} > 0\},\\
R_6 &:= \{(x,y) \in R_C | xN < 0, P_+ > 0, P_- > 0, xH < 0, xy < 0\},
\end{aligned}$$

$$\begin{aligned}
R_7 &:= \{(x,y) \in R_C | N < 0, P_+ < 0, xP_- > 0, xH < 0, y < 0\},\\
R_8 &:= \{(x,y) \in R_C | N < 0, P_+ < 0, P_- > 0, H > 0, x > 0\},\\
R_9 &:= \{(x,y) \in R_C | N > 0, P_+ > 0, P_- < 0, H > 0, x > 0\},\\
R_{10} &:= \{(x,y) \in R_C | N > 0, xP_+ > 0, xH < 0, y > 0\},\\
R_{11} &:= \{(x,y) \in R_C | N < 0, P_+ > 0, H > 0, L_{+,+} < 0\},\\
R_{12} &:= \{(x,y) \in R_C | xN > 0, P_+ > 0, P_- > 0, xH > 0, xy > 0\},
\end{aligned}$$

$$R_{13} := \{(x,y) \in R_C | N < 0, xP_+ < 0, P_- < 0, xH > 0, y > 0\},$$
$$R_{14} := \{(x,y) \in R_C | N < 0, P_+ > 0, P_- < 0, H > 0, x < 0\},$$
$$R_{15} := \{(x,y) \in R_C | N > 0, P_+ < 0, P_- > 0, H > 0, x < 0\},$$
$$R_{16} := \{(x,y) \in R_C | N > 0, xP_- < 0, xH > 0, y < 0\},$$
$$R_{17} := \{(x,y) \in R_C | N < 0, P_- > 0, H > 0, L_{+,-} > 0\},$$
$$R_{18} := \{(x,y) \in R_C | xN < 0, P_+ > 0, P_- > 0, xH < 0, xy > 0\},$$

$$R_{19} := \{(x,y) \in R_C | N < 0, xP_+ > 0, P_- < 0, xH < 0, y > 0\},$$
$$R_{20} := \{(x,y) \in R_C | N < 0, P_+ > 0, P_- < 0, H > 0, x > 0\},$$
$$R_{21} := \{(x,y) \in R_C | N > 0, P_+ < 0, P_- > 0, H > 0, x > 0\},$$
$$R_{22} := \{(x,y) \in R_C | N > 0, xP_- > 0, xH < 0, y < 0\},$$
$$R_{23} := \{(x,y) \in R_C | N < 0, P_- > 0, H > 0, L_{-,+} < 0\},$$
$$R_{24} := \{(x,y) \in R_C | xN > 0, P_+ > 0, P_- > 0, xH > 0, xy < 0\},$$

To continue the analysis, let us examine the images of each partition R_i of the cross, under the map G. The following proposition provides the desired description.

Proposition 4. *For $i \in \{1,2,3,4,5,6\}$,*

1. $G(R_i) = G(R_{i+6}) = R_{13-2i+1} \cup R_{13-2i}$.
2. $G(R_{i+12}) = G(R_{i+18}) = R_{25-2i+1} \cup R_{25-2i}$.

The curve I_c consists of two components, I_c^1 and I_c^2, each being the reflection of the other around horizontal axis, as illustrated in Figure 5. For visual clarity, one of these components, I_2^1, shown in Figure 5a, is further subdivided into two parts, as depicted in Figure 6, which happen to be the reflections of each other around the vertical axis.

Observe that the component I_c^1 fully reside in the union of regions R_1 through R_{12}, and the component I_c^2 fully reside in the union of regions R_{13} through R_{24}.

Now let us partition the curve I_c into 24 segments labeled C_1 through C_{24}, using the regions R_1 through R_{24}, where each C_i is the segment of the curve I_c in the region R_i. This partitioning will be used to analyze the image of each segment, as presented in the following proposition, which indicates that the collection $\{C_i\}$ is a Markov partition for I_c^j, for any $c > 0$ and $j \in \{0,1\}$.

Proposition 5. *For $i \in \{1,2,3,4,5,6\}$, $G(C_i) = G(C_{i+6}) = C_{13-2i+1} \cup C_{13-2i}$ and $G(C_{i+12}) = G(C_{i+18}) = C_{25-2i+1} \cup C_{25-2i}$.*

The Proposition 5 is a direct consequence of Proposition 4. Figure 7 illustrates the G–images of the components C_i described in Proposition 5. Vertical arrows denote the action of G, and the pairs labeled $\overbrace{\underbrace{C_i\,C_j}}$ indicate the resulting images after the application of the action of G.

3 Dynamics of the map G on the level curves

We now restrict the map G to the component I_c^j of the invariant curve I_c, where $j \in \{1,2\}$. By Proposition 5, the partition $\mathcal{C}$ of I_c^j defined in the previous section forms a Markov partition for I_c^j.

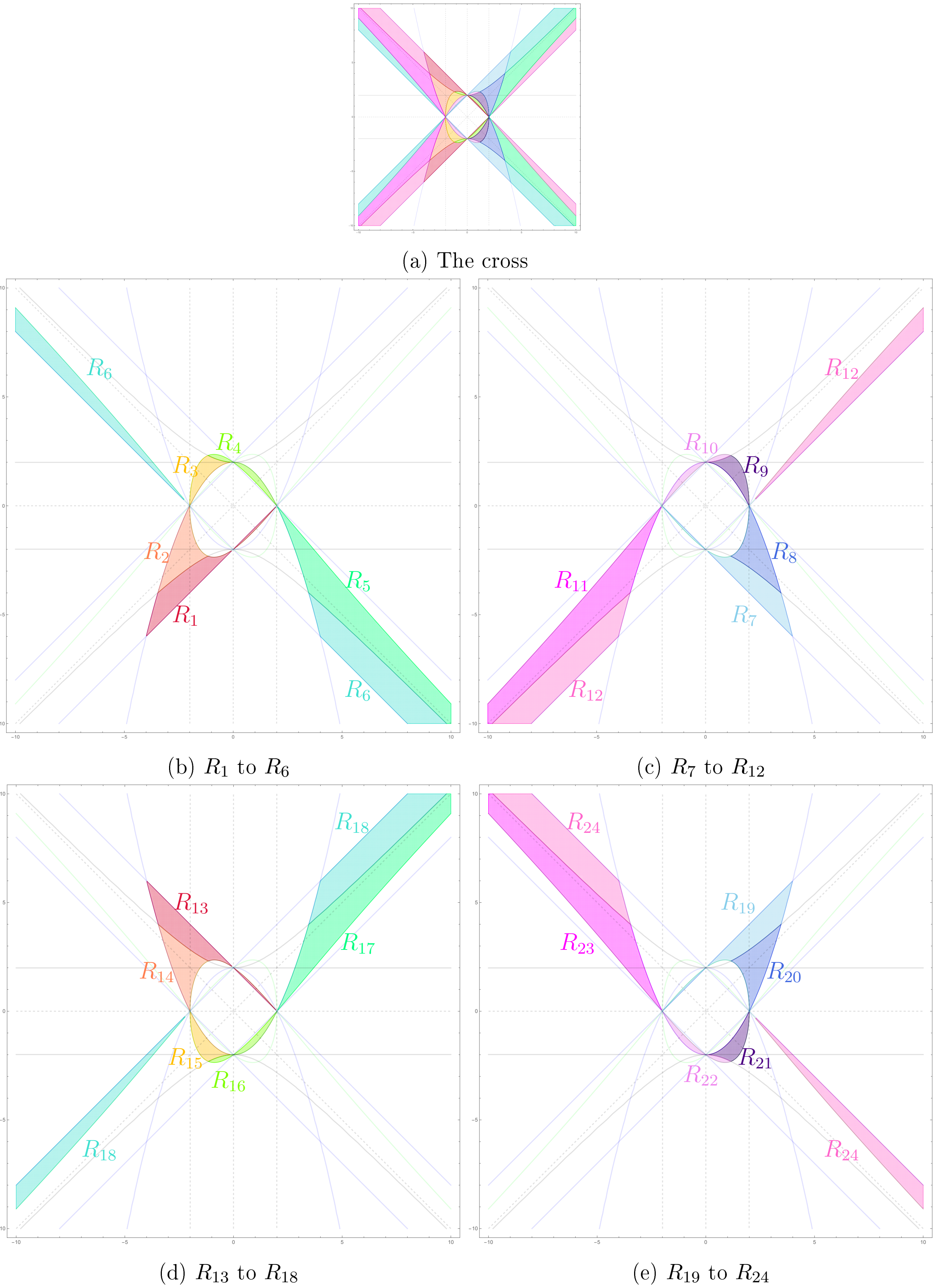

(a) The cross

(b) R_1 to R_6

(c) R_7 to R_{12}

(d) R_{13} to R_{18}

(e) R_{19} to R_{24}

Figure 4: Partition of the cross R_C.

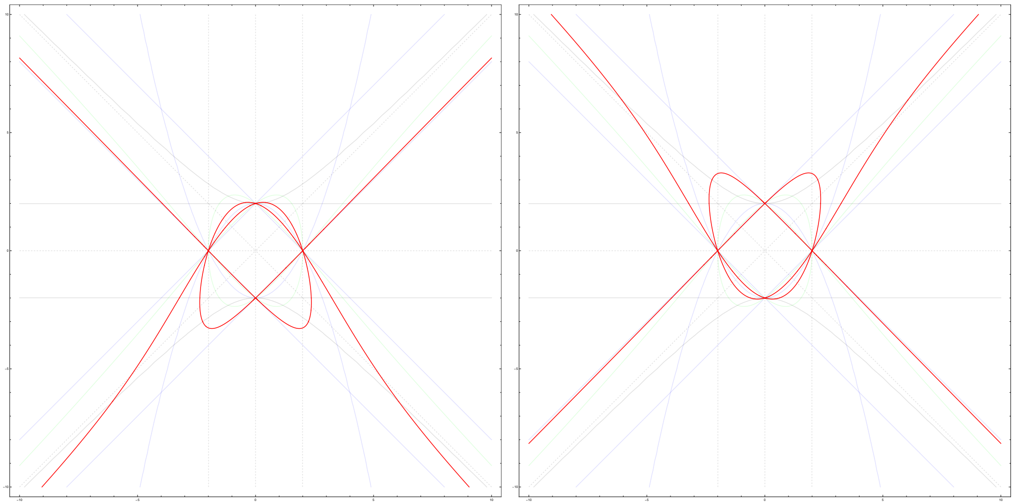

(a) I_2^1 (b) I_2^2

Figure 5: Dividing the curve $I = 2$ into two components.

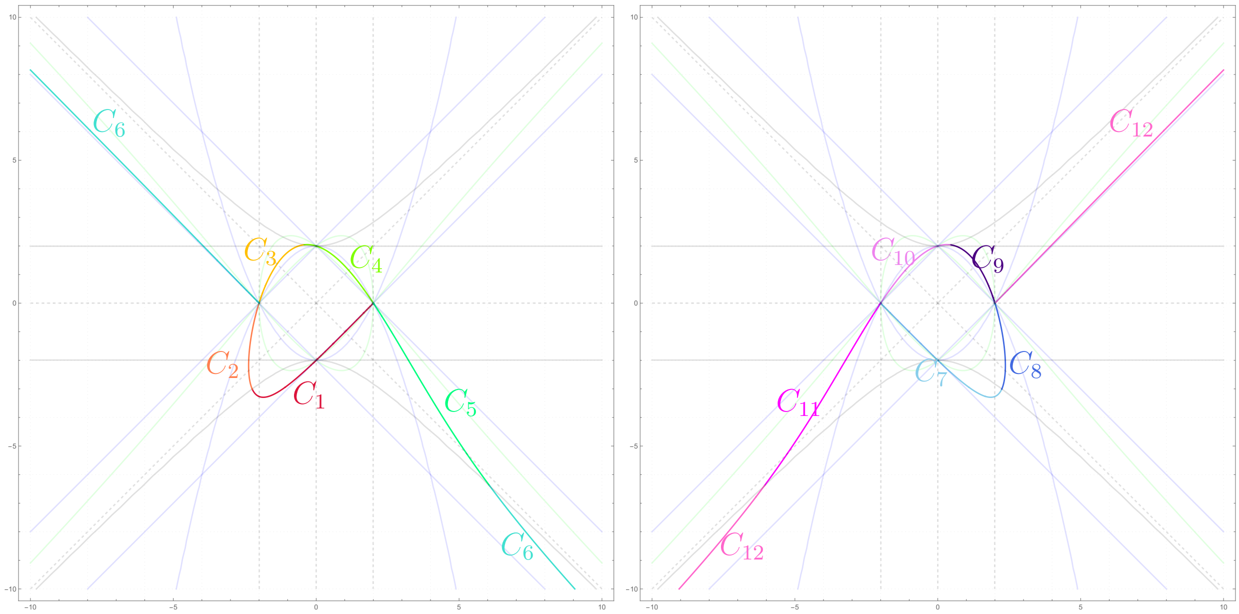

(a) (b)

Figure 6: Dividing the curves I_2^1 in Figure 5a into 12 sub–components. These partitions are formed by the curve's intersections with the hyperbola $H = 0$, and the points $(2, 0)$, $(-2, 0)$.

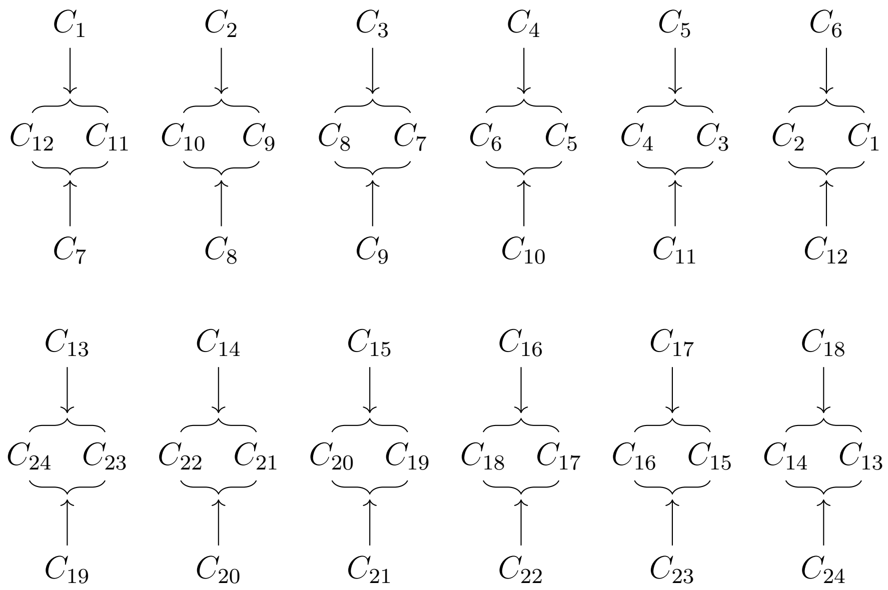

Figure 7: The G–images of components $C_1, \dots, C_{24}$

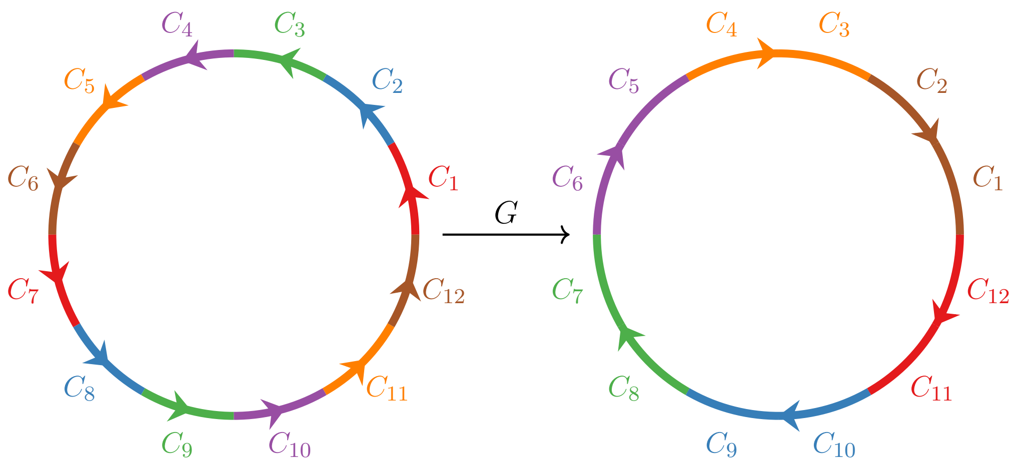

Figure 8: Map G on the component I_c^1 of the invariant curve I_c acts as a double cover with reverse orientation.

When restricted to this curve, the map G acts as a degree–two covering with reversed orientation (see Figure 8). In particular, this implies that the restriction $G|_{I_c^j}$ is an expanding map.

As a consequence of this expanding Markov structure, each point on the curve I_c^j can be uniquely encoded by an infinite symbolic sequence drawn from the alphabet $\mathcal{C}$. This identification is obtained as follows. Given a point $p \in I_c^j$, consider its forward orbit under iteration of G,

$$\left(p, G(p), G^{(2)}(p), G^{(3)}(p), \ldots\right).$$

Since I_c^j is G–invariant, every iterate $G^{(n)}(p)$ lies on I_c^j. For each $n \geq 0$, there exists a unique element $C_{i_n} \in \mathcal{C}$ such that $G^{(n)}(p) \in C_{i_n}$. In this way, the orbit of p determines a symbolic itinerary $(C_{i_0}, C_{i_1}, C_{i_2}, \ldots) \in \mathcal{C}^{\mathbb{N}}$. Let us denote this identification as $h\colon I_C^j \to \mathcal{C}^{\mathbb{N}}$.

Now consider the space $\mathcal{C}^{\mathbb{N}}$ equipped with the shift map σ, defined by

$$\sigma\left((C_{i_n})_{n\geq 0}\right) = (C_{i_{n+1}})_{n\geq 0}.$$

For a point $p \in I_c^j$, let $h(p) = (C_{i_n})_{n\geq 0}$ denote its symbolic itinerary. Then

$$h(G(p)) = (C_{i_{n+1}})_{n\geq 0} = \sigma\left((C_{i_n})_{n\geq 0}\right).$$

Indeed, the $(n+1)$th coordinate of $h(p)$ being $C_{i_{n+1}}$ is equivalent to the condition $G^{(n+1)}(p) \in C_{i_{n+1}}$, which in turn is equivalent to $G^{(n)}(G(p)) \in C_{i_{n+1}}$. This shows that the nth coordinate of $h(G(p))$ is precisely $C_{i_{n+1}}$. Consequently, we obtain

$$\sigma \circ h(p) = h \circ G(p),$$

for all $p \in I_c^j$, consequently proving that the map G is semiconjugate to σ. The relation above can be represented by the following commuting diagram.

$$\begin{array}{ccc} I_c^j & \xrightarrow{G} & I_c^j \\ \big\downarrow h & & \big\downarrow h \\ \mathcal{C}^{\mathbb{N}} & \xrightarrow{\sigma} & \mathcal{C}^{\mathbb{N}} \end{array}$$

Observe that $h(I_c^j)$ is a Markov subshift of finite type of the full shift $\mathcal{C}^{\mathbb{N}}$. The shift map σ acts on this subshift as a degree-two covering with reversed orientation. Consequently, the shift dynamics is conjugate to the anti-holomorphic map $z \mapsto \bar{z}^2$. Since the map G is semiconjugate to the shift map σ via the coding map h, it follows that G is semiconjugate to the ani–holomorphic map $z \mapsto \bar{z}^2$.

4 CONCLUDING REMARKS

We have seen that the map G admits a family of invariant curves, and that the restriction of G to any such invariant curve is semiconjugate to the anti–holomorphic map $z \mapsto \bar{z}^2$. Further investigation is required to determine whether an equidistribution result can be established for G, as well as to study the associated Green current. Moreover, this line of inquiry naturally extends to the setting of higher–dimensional rational maps that generalize the map G, where similar dynamical phenomena may arise.

References

[1] Bartholdi L., Grigorchuk R.I. *Spectra of non-commutative dynamical systems and graphs related to fractal groups.* C. R. Acad. Sci. Paris Sér. I Math. 2000, **331** (6), 429–434. doi:10.1016/S0764-4442(00)01658-X

[2] Bartholdi L., Grigorchuk R.I. *On the spectrum of Hecke type operators related to some fractal groups.* Tr. Mat. Inst. Steklova 2000, **231**, 5–45. (in Russian)

[3] Bartholdi L., Virág B. *Amenability via random walks.* Duke Math. J. 2005, **130** (1), 39–56. doi:10.1215/S0012-7094-05-13012-5

[4] Dang N.B., Grigorchuk R.I., Lyubich M. *Self-similar groups and holomorphic dynamics: renormalization, integrability, and spectrum.* Arnold Math. J. 2023, **9** (4), 505–597. doi:10.1007/s40598-022-00223-0

[5] Pierre Fatou. *?uvres mathŭmatiques.* Centre National de la Recherche Scientifique, 1964. Originally published works from 1917–1920 on iteration of rational functions.

[6] Grigorchuk R.I., Nekrashevych V. *Self-similar groups, operator algebras and Schur complement.* J. Mod. Dyn. 2007, **1** (3), 323–370. doi:10.3934/jmd.2007.1.323

[7] Grigorchuk R.I., Nekrashevych V., Šunić Z. *From self-similar groups to self-similar sets and spectra.* In: Fractal geometry and stochastics V, Progr. Probab. **70**, 175–207, Birkhäuser/Springer, Cham, 2015.

[8] Grigorchuk R.I., Samarakoon S.T. *Integrable and chaotic systems associated with fractal groups.* Entropy Feb 2021, **23** (2), 237. doi:10.3390/e23020237

[9] Grigorchuk R.I. *On Burnside's problem on periodic groups.* Funktsional. Anal. i Prilozhen. 1980, **14** (1), 53–54.

[10] Grigorchuk R.I. *On the Milnor problem of group growth.* Dokl. Akad. Nauk SSSR 1983, **271** (1), 30–33.

[11] Grigorchuk R.I. *On growth in group theory.* In: Proceedings of the International Congress of Mathematicians, Vol. I, II (Kyoto, 1990), Math. Soc. 325–338, Japan, Tokyo, 1991.

[12] Julia G. *Mémoire sur l'itération des fonctions rationnelles.* J. Math. Pures Appl. 1918, **8**, 47–245. (in French)

[13] Kaimanovich V.A. *"Münchhausen trick" and amenability of self-similar groups.* Internat. J. Algebra Comput. 2005, **15** (5–6), 907–937. doi:10.1142/S0218196705002694

[14] McMullen C.T. Complex Dynamics and Renormalization. In: Annals of Mathematics Studies, 135. Princeton University Press, Princeton, NJ, 1994.

[15] Milnor J. Advanced problems: 5603. Amer. Math. Monthly 1968, **75** (6), 685–686.

[16] Milnor J. Dynamics in One Complex Variable. In: Annals of Mathematics Studies, 160 (3). Princeton University Press, Princeton, NJ, 2006.

[17] Nekrashevych V. Self-Similar Groups In: Mathematical Surveys and Monographs, 117. American Mathematical Society, Providence, RI, 2005.

[18] Sabot C. *Spectral properties of self-similar lattices and iteration of rational maps.* Mém. Soc. Math. Fr. (N.S.) 2003, (92), vi+104. doi:10.24033/msmf.405 (in French)

[19] Silverman J.H. The Arithmetic of Dynamical Systems. In: Graduate Texts in Mathematics, 241. Springer, New York, 2007.

[20] Švarc A.S. *A volume invariant of coverings.* Dokl. Akad. Nauk SSSR (N.S.) 1955, **105**, 32–34. (in Russian)

[21] Teplyaev A. *Spectral analysis on infinite sierpiński gasket.* J. Funct. Anal. 1998, **159** (2), 537–567. doi:10.1006/jfan.1998.3297

[22] Yang R. *Projective spectrum in Banach algebras.* J. Topol. Anal. 2009, **1** (3), 289–306. doi:10.1142/S1793525309000126

Received 01.12.2025

Grigorchuk R.I., Samarakoon S.T., Vorobets Y. (in Ukrainian) *На другій двовимірній раціональній карті, пов'язаній з першою групою проміжного зростання.* // Буковинський матем. журнал — 2025. — Т.13, №2. — С. 188–200.

Ми показуємо, що друге раціональне відображення G, пов'язане з групою $\mathcal{G}$ проміжного зростання, побудованою першим автором у 1980 році, є напівспряженим з антиголоморфним відображенням $z \to \bar{z}^2$. Для цього ми використовуємо сімейство G–інваріантних кривих, знайдених третім автором, і для кожної інваріантної кривої створюємо її марковське розбиття.